Additionally, methyl-β-cyclodextrin (M-β-CyD) is acknowledged to disrupt the structures of lipid rafts and caveolae (Galbiati et al., 2001), which are lipid microdomains formed by lateral assemblies of cholesterol and sphingolipids in the cell membrane, through the extraction of cholesterol from the microdomains (Anderson and Jacobson, 2002). Furthermore, we demonstrated that 2,6-di-O-methyl-β-cyclodextrin (DM-β-CyD) induced apoptosis through the inhibition of PI3K-Akt-Bad pathway, leading to cholesterol depletion from lipid rafts in NR8383 cells, a rat alveolar macrophage cell line (Motoyama et al., 2009a). However, it is still not unclear whether M-β-CyD induces apoptosis or not through the interaction with membrane components in various tumor cells. Meanwhile, we previously revealed that the membrane interaction mode of M-β-CyD was somewhat different from that of DM-β-CyD (Motoyama et al., 2009a). Actually, M-β-CyD extracts cholesterol from cell membranes, while it interacts with phospholipids only very slightly. Meanwhile, DM-β-CyD has the potent cholesterol and phospholipids extraction ability from plasma membrane of cells. Due to the different interaction mode of M-β-CyD, compared to DM-β-CyD, against cell membrane components, in the present study, we therefore examined whether cell-death induced by M-β-CyD is apoptosis or not in various cells, and evaluated the potential of M-β-CyD as an antitumor agent *in vivo*.

2. Materials and methods

2.1. Materials

M-β-CyD with an average degree of substitution (DS) of methyl group of 12.2 was obtained from Junsei Chemical (Tokyo, Japan). RPMI-1640 culture medium (folic acid (FA)-free) was purchased from GIBCO (Tokyo, Japan). Dulbecco's modified Eagle's medium (DMEM) and fetal bovine serum (FBS) were purchased from Nissui Pharmaceuticals (Tokyo, Japan) and Nichirei (Tokyo, Japan), respectively. Tetramethylrhodamine isothiocyanate (TRITC) was obtained from Funakoshi (Tokyo, Japan). CellEvent™ Caspase-3/7 Green Detection Reagent and Cyto-ID™ Autophagy Detection Kit were purchased from Invitrogen (Tokyo, Japan) and Enzo Life Sciences (Farmingdale, NY), respectively. All other chemicals and solvents were of analytical reagent grade, and deionized double-distilled water was used throughout the study.

2.2. Cell culture

KB cells through referred to as a human oral squamous carcinoma cell line, which is now known to be a subline of the ubiquitous KERATIN-forming tumor cell line HeLa, were cultured as reported previously (Onodera et al., 2011). Ihara cells, a highly pigmented human melanoma cell line, and M213 cells, a human cholangiocarcinoma cell line, were grown in DMEM-high glucose containing glucose (4.5 mg/mL), penicillin (1×10^5 mU/mL) and streptomycin (0.1 mg/mL) supplemented with 10% FBS at 37 °C in a humidified 5% CO_2 and 95% air atmosphere.

2.3. In vitro cytotoxic activity

In vitro cytotoxic activity was assayed by the WST-1 method (a Cell Counting Kit, Wako Pure Chemical Industries, Osaka, Japan). Briefly, KB cells, Ihara cells, and M213 cells were seeded at 5×10^4 cells onto 24-well microplate (Iwaki, Tokyo, Japan) and incubated for 24 h in a humidified atmosphere of 5% CO_2 and 95% air at 37 °C. Cells were washed twice with culture medium, and then incubated with 300 μL of culture medium containing 20 mM M-β-CyD in the presence or absence of cholesterol for 2 h at 37 °C. In the cholesterol-loading experiment, we used saturated cholesterol in culture medium obtained by 24 h after shaking with 5 mg of cholesterol and 20 mM M-β-CyD and filtering them. After washing twice with phosphate-buffered saline (PBS, pH 7.4) to remove M-β-CyD, 300 μL of fresh Hanks' balanced salt solution (HBSS, pH 7.4) and 30 μL of WST-1 reagent were added to the plates and incubated for 30 min at 37 °C. The absorbance at 450 nm against a reference wavelength of 630 nm was measured with a microplate reader (Bio-Rad Model 550, Tokyo, Japan).

2.4. Cellular association of M-β-CyD

KB cells, Ihara cells and M213 cells (1×10^6/35 mm dish) were incubated with 1 mL of culture medium containing 10 μM TRITC-labeled M-β-CyD (TRITC-M-β-CyD) at 37 °C for 1 h. After washing twice with 1 mL of PBS (pH 7.4) to remove the sample, and immediately scraped with 1 mL of PBS (pH 7.4). The cells were collected and filtered through nylon mesh. Data were collected for 1×10^4 cells on a FACSCalibur flow cytometer using CellQuest software (Becton-Dickinson, Mountain View, CA).

2.5. Intracellular distribution of M-β-CyD

KB cells (1×10^6/35 mm glass bottom dish) were incubated with 10 μM TRITC-M-β-CyD at 37 °C for 1 h. After incubation, Hoechst 33342 (10 μg/mL) was added to each well and incubated at 37 °C for 10 min. The cells were washed with RPMI-1640 culture medium (FA-free) twice, and were added 1 mL of RPMI-1640 culture medium (FA-free). The cells were observed by a fluorescence microscope (KEYENCE Biozero BZ-8000, Tokyo, Japan).

2.6. Determination of cholesterol in the culture medium

KB cells (1×10^6/35 mm dish) were incubated with 20 mM M-β-CyD in RPMI-1640 culture medium (FA-free) at 37 °C for 1 h. After centrifugation (10,000 rpm, 5 min) of the culture medium, the supernatant was recovered. Total cholesterol in the culture medium was determined using a Cholesterol-test Wako® (Wako Pure Chemical Industries, Osaka, Japan).

2.7. DNA content

For determination of DNA content in cells, KB cells (1×10^6/35 mm dish) were incubated with RPMI-1640 culture medium (FA-free) containing 20 mM M-β-CyD for 2 h. After washing with PBS, the cells were suspended and fixed with 500 μL of ice-cold 70% (v/v) ethanol for 4 h. After washing with PBS and subsequent centrifugation, cells were re-suspended with RNase A (100 μg/ml) and incubated for 30 min at 37 °C. After centrifugation, cells were resuspended in a solution containing 500 μL of propidium iodide (PI, 20 μg/mL) and incubated for 20 min on ice before quantification using a FACSCalibur flow cytometer with CellQuest software (Becton Dickinson, Mountain View, CA).

2.8. Mitochondrial transmembrane potential

To measure the mitochondrial transmembrane potential, rhodamine 123 was used as reported previously (Motoyama et al., 2009a). KB cells (1×10^6/35 mm dish) were incubated with RPMI-1640 culture medium (FA-free) containing 20 mM M-β-CyD for 2 h. After washed with PBS, cells were stained by 10 μM rhodamine 123 for 15 min at 37 °C. After washing once with 1 mL of PBS to remove the samples, cells were lysed by the addition of 1 mL of PBS. Then, mitochondrial transmembrane potential was analyzed by a FACSCalibur flow cytometer as described above.

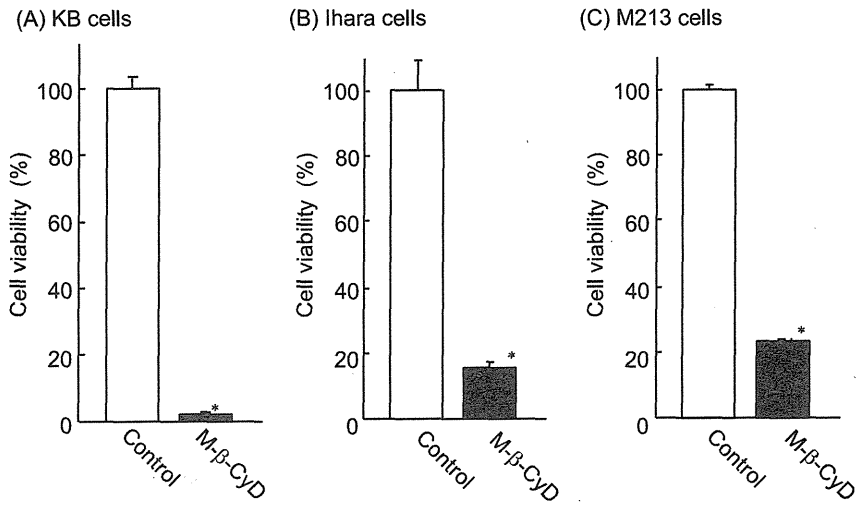

Fig. 1. Cytotoxic activity of M-β-CyD in various cells. (A) KB cells, (B) Ihara cells, and (C) M213 cells were incubated for 2 h with 300 μL of medium containing M-β-CyD (20 mM) at 37 °C. After washing twice with PBS to remove M-β-CyD, 300 μL of fresh HBSS and 30 μL of WST-1 reagent were added to plates and incubated for 30 min at 37 °C. Each value represents the mean ± S.E.M. of 3–4 experiments. *$p < 0.05$, compared with control.

2.9. Activation of caspase-3/7

KB cells (1×10^6/35 mm dish) were incubated with 20 mM M-β-CyD for 2 h. After washing twice with 1 mL of RPMI-1640 (FA-free) medium to remove the samples, cells were add to 10 μM CellEvent™ Caspase-3/7 Green Detection Reagent (Invitrogen, Tokyo, Japan) and incubated at 37 °C for 30 min. The cells were washed with RPMI-1640 (FA-free) medium twice, and added 1 mL of RPMI-1640 (FA-free) medium. The cells were observed by a fluorescence microscope (KEYENCE Biozero BZ-8000, Tokyo, Japan).

2.10. Detection of autophagosome

Cyto-ID™ Autophagy Detection Kit was used for determination of autophagic vacuoles in cells using a novel dye that selectively labels autophagic vacuoles. Briefly, the cells (1×10^6/35 mm glass bottom dish) were incubated with RPMI-1640 culture medium for 24 h. After washing with PBS, the cells were incubated with 20 mM M-β-CyD for 2 h, and then the cells were treated with Cyto-ID™ Autophagy Detection Kit. After washing with RPMI-1640 culture medium, the cells were observed by a fluorescence microscope (KEYENCE Biozero BZ-8000, Tokyo, Japan).

2.11. Evaluation of antitumor effect of M-β-CyD

Four-weeks-old BALB/c male mice (*ca.* 20 g) were subcutaneously injected the suspension containing Colon-26 carcinoma cells (5×10^5 cells/100 μL), FR-α expressing cells on a hind leg. About 10 days later, the mannitol solution (5%) dissolved with M-β-CyD (10, 50, or 100 mg/kg) was administered by the single intratumoral injection to tumor bearing mice. The tumor volumes were determined by the equation (Volume = $LW^2/2$), where L is the longest dimension parallel to the skin surface and W is the dimension perpendicular to L and parallel to the surface. The body weight changes of tumor-bearing mice were monitored for 21 days. Animal experiments were approved by the Ethics Committee for Animal Care and Use of Kumamoto University (Approval ID: 24-286).

2.12. Data analysis

Data are given as the mean ± S.E.M. Statistical significance of mean coefficients for the studies was performed by analysis of variance followed by Scheffe's test. *p*-Values for significance were set at 0.05.

3. Results

3.1. Cytotoxic activity of M-β-CyD

To examine the cytotoxic activity of M-β-CyD, the cell viability of various tumor cells was determined by WST-1 method. In our previous study, the cytotoxic activity of 10 mM M-β-CyD for 2 h was somewhat weak. Therefore, 20 mM M-β-CyD was treated for 2 h in cytotoxic study. M-β-CyD had potent cytotoxic activity, compared to control, in KB cells, Ihara cells and M213 cells, after treatment for 2 h (Fig. 1A–C). These results suggest that M-β-CyD had potent cytotoxic activity.

3.2. Cellular association and intracellular distribution of M-β-CyD

To gain insight into the mechanism for the cytotoxic activity of M-β-CyD, we examined the cellular association of TRITC-M-β-CyD after treatment for 1 h with various cells (Fig. 2). Herein the incubation time of M-β-CyD was set for 1 h, because KB cells could not survive for more than 2 h. TRITC-M-β-CyD associated with neither KB cells, Ihara cells, nor M213 cells (Fig. 2B–D). Additionally, we investigated the intracellular distribution of TRITC-M-β-CyD in KB cells after 1 h treatment using a fluorescent microscope (Fig. 2E). In consistent with the results of Fig. 2B, cellular uptake of TRITC-M-β-CyD in KB cells was not observed, compared to that of rhodamin123 as a positive control (Fig. 2A). Collectively, these results suggest that M-β-CyD was biomembrane-impermeable.

3.3. Effect of cholesterol extraction ability on cytotoxic activity of M-β-CyD

Lipid rafts are mainly composed of cholesterol and sphingolipids in the cell membranes, and contain various signal transduction molecules including growth factor receptors (Le Roy and Wrana, 2005). We previously reported that CyDs showed hemolytic activity at high concentration through the extraction of cell membrane components such as cholesterol and phospholipids from lipid rafts (Motoyama et al., 2006; Ohtani et al., 1989). Furthermore, we

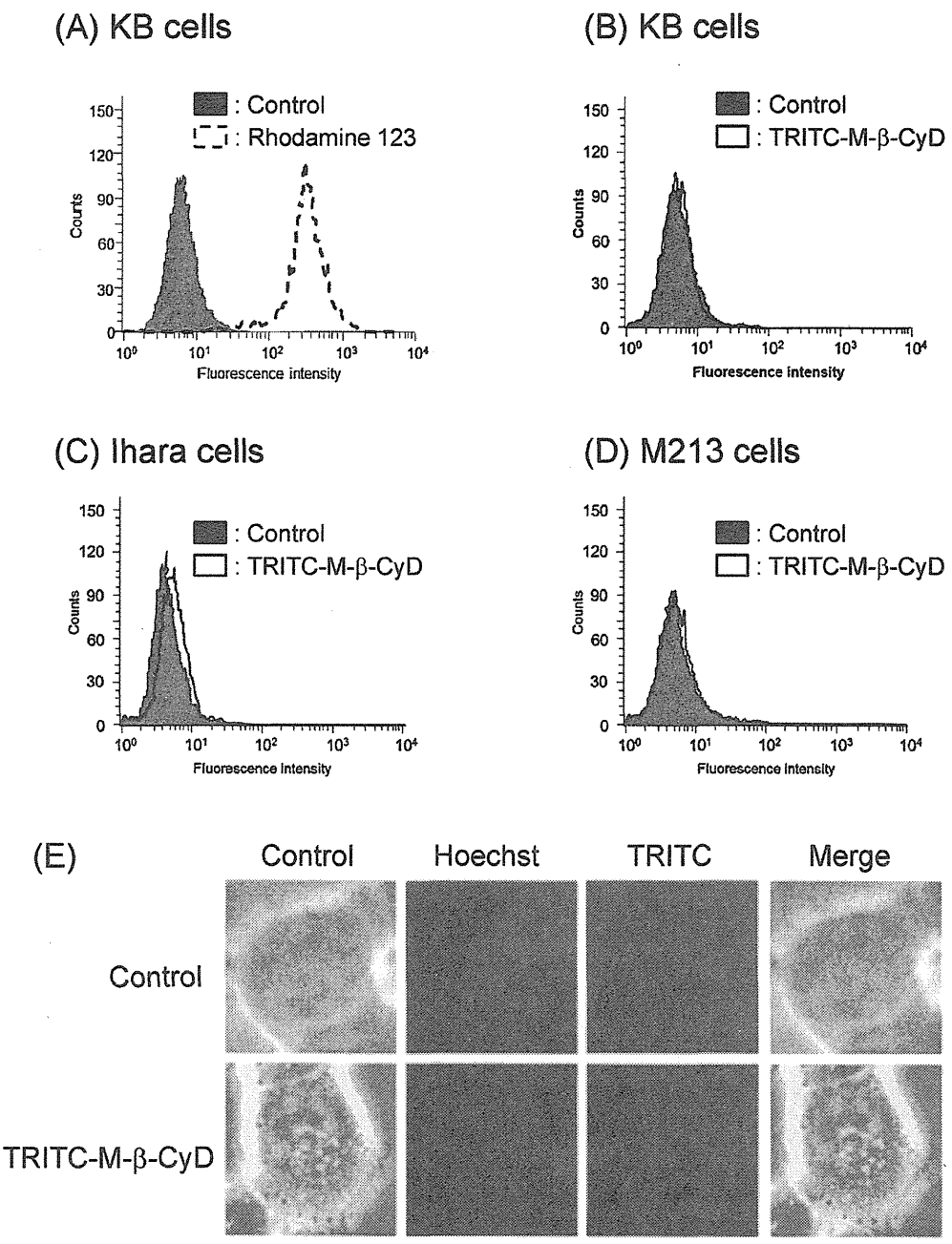

Fig. 2. Cellular association of TRITC-M-β-CyD in various cells. The fluorescence intensities of (A) rhodamine 123 in KB cells and TRITC in (B) KB cells, (C) Ihara cells, and (D) M213 cells were determined 1 h after incubation at 37 °C by a flow cytometer. (E) Intracellular distribution of TRITC-M-β-CyD in KB cells after treatment for 1 h. The experiments were performed independently three times, and representative data are shown.

demonstrated that DM-β-CyD induces apoptosis through cholesterol depletion in NR8383 cells (Motoyama et al., 2009a). Therefore, to reveal whether cell-death induced by M-β-CyD is apoptosis through cholesterol depletion in tumor cells, we investigated the effects of M-β-CyD on the release of cholesterol from KB cells to culture medium. Cholesterol released in the culture medium after incubation with 20 mM M-β-CyD for 1 h was determined by Cholesterol-test Wako®. The extent of cholesterol efflux by M-β-CyD was significantly higher than that of control in KB cells (Fig. 3).

Next, to confirm the involvement of cholesterol depletion in cell-death induced by M-β-CyD, we examined the cell viability of KB cells in the cholesterol-loaded medium containing M-β-CyD. Importantly, the cytotoxic activity of M-β-CyD in KB cells was significantly lowered in saturated cholesterol-loading culture medium (Fig. 4). Taken together, these results suggest that the extraction ability of M-β-CyD on cholesterol from plasma membranes may be associated with the cytotoxic activity in KB cells.

3.4. M-β-CyD caused cell-death in apoptosis-dependent pathway

To investigate whether M-β-CyD-induced cell-death is accompanied by apoptotic feature, we next examined the DNA content in nucleus, mitochondrial transmembrane potential, and caspase-3/7 activity in KB cells (Fig. 5). The DNA content in nucleus after incubation with 20 mM M-β-CyD for 2 h was strikingly decreased compared to that with control (without CyD) in KB cells (Fig. 5A).

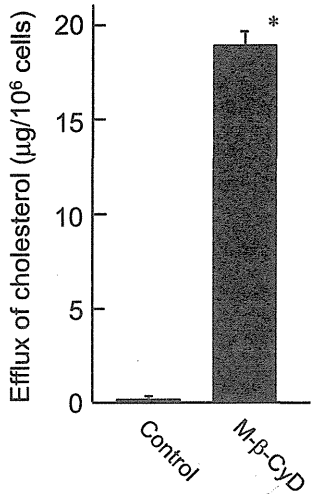

Fig. 3. Efflux of cholesterol from lipid rafts to culture medium after treatment with M-β-CyD (20 mM) in KB cells. Each value represents the mean ± S.E.M. of 3–4 experiments. $^{*}p < 0.05$, compared with control.

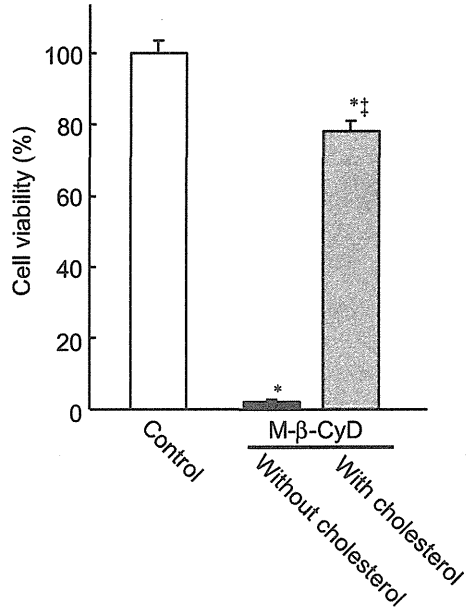

Fig. 4. Effect of cholesterol on cytotoxic activity of M-β-CyD (20 mM) in KB cells. Each value represents the mean ± S.E.M. of 6–9 experiments. $^{*}p < 0.05$, compared with control. $^{\ddagger}p < 0.05$, compared with M-β-CyD without cholesterol.

Next, we studied the effects of CyDs on mitochondrial transmembrane potential using rhodamine 123 in KB cells (Fig. 5B). The mitochondrial transmembrane potential of KB cells treated with M-β-CyD was significantly decreased, compared to that with control (without CyD).

Activation of caspase-3/7 is considered an essential event during apoptosis. We next examined the caspase-3/7 activity in KB cells after treatment with M-β-CyD using the CellEvent™ Caspase-3/7 Green Detection Reagent (Fig. 5C). This caspase-3/7 detection reagent is intrinsically non-fluorescent as the DEVD peptide inhibits the ability of the dye to bind to DNA. However, after activation of caspase-3/7 in apoptotic cells, the DEVD peptide is cleaved and enabled the dye to bind to DNA and produce a bright, fluorogenic response. Treatment of KB cells with M-β-CyD

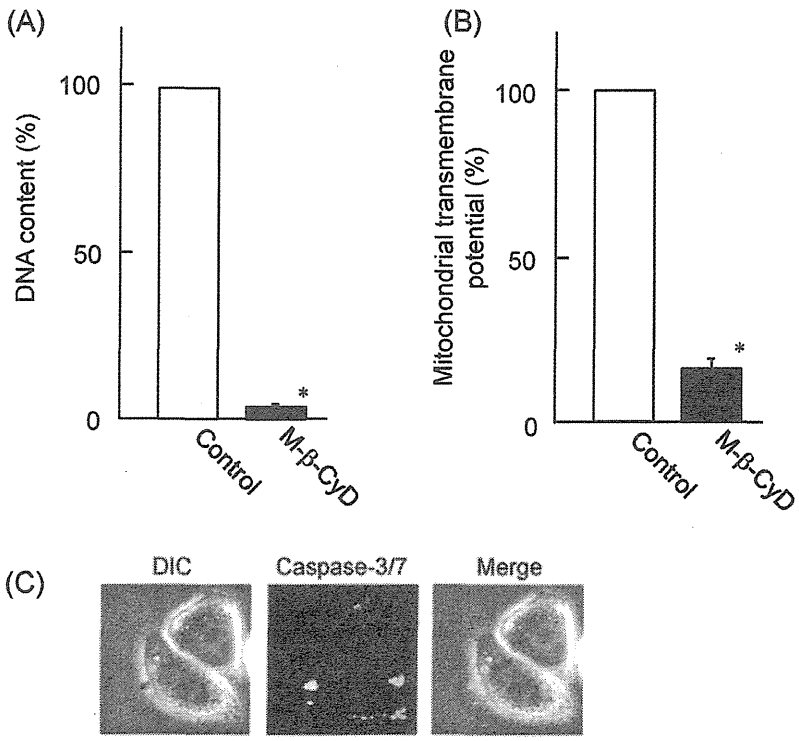

Fig. 5. Induction of apoptosis, but not autophagy, in KB cells after treatment with M-β-CyD. Effects of M-β-CyD on DNA content (A) and mitochondrial transmembrane potential (B). KB cells were treated with M-β-CyD (20 mM) for 2 h. Each value represents the mean ± S.E.M. of 3–4 experiments. $^{*}p < 0.05$, compared with control. (C) Caspase-3/7 activity in KB cells after treatment with M-β-CyD. The experiments were performed independently three times, and representative images are shown.

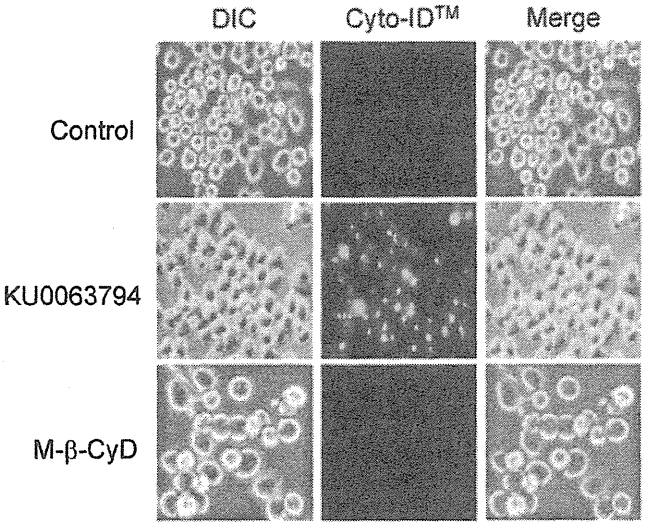

Fig. 6. Effects of M-β-CyD on the formation of autophagosomes in KB cells. KB cells were treated with M-β-CyD (20 mM) for 2 h, and then the cells were treated with Cyto-ID™. The concentration of KU0063794, an autophagy inducer, was 10 μM. After washed twice with PRMI medium (FA (+)), cells were scanned with a fluorescence microscope. The experiments were performed independently three times, and representative images are shown.

for 2 h caused caspase-3/7 activation (Fig. 5C). Collectively, these results strongly suggest that M-β-CyD caused cell-death in KB cells in apoptosis-dependent pathway.

Autophagy can promote cell adaptation and survival, but under some conditions it leads to cell-death. A number of studies have reported that autophagy or autophagic cell-death is activated in cancer cells that are derived from tissues such as breast, colon, prostate and brain, in response to various anticancer therapies (Kondo et al., 2005). Therefore, we investigated whether M-β-CyD induces autophagic cell-death in KB cells or not, using Cyto-ID™ Autophagy Detection Kit, which measures autophagic vacuoles such as pre-autophagosomes, autophagosomes, and autolysosomes (autophagolysosomes) in live cells. As shown in Fig. 6, the autophagic vacuoles in KB cells did not observe after treatment with M-β-CyD for 2 h. These results suggest that M-β-CyD did not induce autophagic cell-death in KB cells.

3.5. Antitumor activity of M-β-CyD in tumor-bearing mice

To investigate the antitumor activity of M-β-CyD *in vivo*, we injected M-β-CyD solution intratumorally to Colon-26 cells-bearing mice. Here we selected Colon-26 cells for *in vivo* experiments, because the cells express FR-α and are often used as allografted tumor model. As shown in Fig. 7A, an intratumoral injection of the M-β-CyD at a dose of 10, 50, and 100 mg/kg drastically inhibited the tumor growth, compared to that of control (5% mannitol solution). In the viewpoint of safety, the body weight of mice after an intratumoral injection of M-β-CyD was slightly increased as the time passed (Fig. 7B). These results suggest that M-β-CyD had the potent antitumor activity after intratumoral injection to tumor-bearing mice.

4. Discussion

In the present study, we revealed that M-β-CyD potentially caused apoptosis in KB, Ihara and M213 cells, possibly due to cholesterol depletion from lipid rafts, and M-β-CyD drastically inhibited the tumor growth after intratumoral injection to Colon-26 cells-bearing mice.

Generally, it is difficult for CyDs to induce apoptosis after uptake into cells, because CyDs have poor membrane permeability due to its aqueous properties and high molecular weight. Rosenbaum et al. reported, however, that β-CyD/dextran conjugates can enter cells and located cholesterol-enriched lysosomal storage organelles, and were effective at reducing the cholesterol accumulation (Rosenbaum et al., 2010). Additionally, Plazzo et al. also reported that M-β-CyD tagged with fluorescein can be internalized *via* clathrin-dependent endocytosis in HeLa cells. To resolve this controversial, we examined the cellular association of TRITC-M-β-CyD in various cells. As a result, TRITC-M-β-CyD was associated with KB cells, Ihara cell, and M213 cells only very slightly under the present experimental conditions (Fig. 2B–D). Therefore, we hypothesized that apoptosis induced by CyDs is involved in the interaction with plasma membrane components. Actually, non-ionic surfactants, such as polyethylene glycol sorbitan monolaurate (Tween 20), polyoxyethylenehydrogenated caster oil 60 (HCO-60) and Triton X-100, induced apoptosis in NR8383 cells at more than critical micelle concentrations, probably due to the solubilizing effects of cell membrane components such as cholesterol and phospholipids (data not shown). Therefore, it is highly likely that the solubilizing effects of M-β-CyD on membrane lipids resulted in the

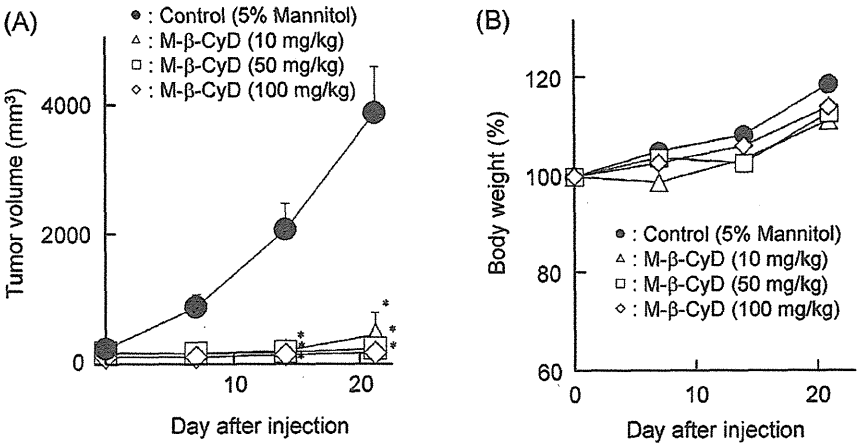

Fig. 7. Effects of intratumoral administration of M-β-CyD on tumor growth (A) and body weight (B) in tumor-bearing mice. The dose of M-β-CyD was 10, 50 or 100 mg/kg. The number of mice for Control, M-β-CyD (10 mg/mL), M-β-CyD (50 mg/mL) and M-β-CyD (100 mg/mL) was 5, 3, 3 and 3, respectively. *$p < 0.05$, compared with control (5% mannitol solution).

induction of apoptosis, because M-β-CyD has high hemolytic activity through the solubilizing effects on cholesterol (Irie and Uekama, 1997, 1999).

Recently, it is reported that lipid rafts, which are lipid microdomains mainly composed of cholesterol and sphingolipids, are contributed to apoptosis *via* FasL/Fas and Bad, an apoptosis inducible factor of Bcl-2 family (Ayllon et al., 2002; Hueber et al., 2002; Legler et al., 2003). In addition, we previously revealed that M-β-CyD extracted cholesterol from lipid microdomains from rabbit red blood cells (Motoyama et al., 2009b). Therefore, we examined whether apoptosis induced by M-β-CyD is contributed to the extraction of cholesterol from lipid rafts. Actually, M-β-CyD significantly released cholesterol from lipid rafts into the culture medium in KB cells (Fig. 3). Moreover, the cytotoxic activity of M-β-CyD was potentially inhibited by the addition of cholesterol in culture medium (Fig. 4). Therefore, these results strongly suggest that cholesterol depletion in lipid rafts had a crucial role in the induction of apoptosis by M-β-CyD. Further elaborate studies on not only the extent of cholesterol after treated with M-β-CyD in cell membranes, but also the relation of extracted cholesterol and cell death should be performed.

PI3K activates Akt through the recruitment of Akt and PDK1 (3-phospho-inositide-dependent protein kinase-1) to lipid rafts caused by production of PI(3,4,5)P3. This activated-Akt by PI3K suppresses the induction of apoptosis through the phosphorylation of Bad and caspase-9. Previously, we demonstrated that DM-β-CyD significantly suppressed phosphorylation of Akt and accelerated degradation of Akt in NR8383 cells through the extraction of cholesterol from lipid rafts (Motoyama et al., 2009a). Furthermore, we revealed that DM-β-CyD potentially suppressed phosphorylation of Bad (Motoyama et al., 2009a). Zha et al. reported that suppression of Bad phosphorylation binds with Bcl-xL, an apoptosis inhibitory factor on mitochondrial cell membrane, resulting in induction of apoptosis (Zha et al., 1996). Therefore, it can be thought that M-β-CyD could suppress the activation of PI3K-Akt-Bad pathway, as well as DM-β-CyD, in apoptotic cell-death induction.

Signal transduction regarding the induction of apoptosis is largely discriminated into a mitochondrial-dependent or -independent pathway. Mitochondrion have crucial roles in signal transduction of apoptosis, because the activation of caspase family is induced through the reduction of mitochondrial transmembrane potential following the release of cytochrome *c* prior to apoptosis. To release cytochrome *c* from mitochondria during apoptosis, the formation of VDAC (voltage-dependent anion channel) tetramer on the mitochondrial membrane plays an important role (Shimizu et al., 2001, 1999). On the other hand, Bcl-xL regulates the release of cytochrome *c* through the suppression of VDAC channel activity (Yang et al., 1995; Zha et al., 1996). As apoptosis induction by Bad is contributed to the binding of Bad with Bcl-xL on the mitochondrial membrane. Previously, we revealed that the inhibition of phosphorylation of Bad by DM-β-CyD induced the collapse of mitochondrial transmembrane potential and released cytochrome *c* from mitochondria (Motoyama et al., 2009a). In the present study, we demonstrated that M-β-CyD lowered the mitochondrial transmembrane potential in KB cells (Fig. 5B). Therefore, apoptosis induced by M-β-CyD was found to be potentially involved in the mitochondria-dependent pathway. In addition to fluorescence staining (Fig. 5C), in order to further confirm the caspase 3/7 activation in KB cells after treatment with M-β-CyD, western blot analysis is thereafter required.

It should be noted that M-β-CyD provided *in vivo* antitumor activity after an intratumoral injection to Colon-26 cells-bearing mice (Fig. 7). Grosse et al. reported that the antiproliferative activity of M-β-CyD was statistically higher than that of doxorubicin after intraperitoneal administrations to Swiss nude mice xenografted with MCF7 or A2789 tumor cells (Grosse et al., 1998). Thus, M-β-CyD is likely to be more preferable to doxorubicin from the viewpoint of both pharmacological effects. However, an intravenous administration of M-β-CyD did not show any significant antitumor activity (data not shown), probably due to the lack of target specificity against tumor cells and rapid renal clearance from body. Therefore, we are currently investigating the *in vitro* and *in vivo* antitumor activity of M-β-CyD modified with folic acid as a tumor targeting ligand, which recognizes by folate receptor-α-overexpressing tumor cells.

In conclusion, the present study may demonstrate that M-β-CyD induced mitochondria-dependent apoptosis through cholesterol depletion in lipid rafts of tumor cells, and had the potential of a novel antitumor agent and/or its lead compound.

Acknowledgements

This work was partially supported by a Grant-in-Aid for Young Scientists (B) from Japan Society for the Promotion of Science (22790040) and by a Grant-in-Aid for Third Term Comprehensive Control Research for Cancer from Ministry of Health Labor and Welfare (24100701). This work was supported by the Sasakawa Scientific Research Grant from The Japan Science Society.

References

Anderson, R.G., Jacobson, K., 2002. A role for lipid shells in targeting proteins to caveolae, rafts, and other lipid domains. Science 296, 1821–1825.
Ashkenazi, A., 2008. Directing cancer cells to self-destruct with pro-apoptotic receptor agonists. Nat. Rev. Drug Discov. 7, 1001–1012.
Ayllon, V., Fleischer, A., Cayla, X., Garcia, A., Rebollo, A., 2002. Segregation of Bad from lipid rafts is implicated in the induction of apoptosis. J. Immunol. 168, 3387–3393.
Burger, K., Gimpl, G., Fahrenholz, F., 2000. Regulation of receptor function by cholesterol. Cell Mol. Life Sci. 57, 1577–1592.
Galbiati, F., Razani, B., Lisanti, M.P., 2001. Emerging themes in lipid rafts and caveolae. Cell 106, 403–411.
Grosse, P.Y., Bressolle, F., Pinguet, F., 1998. Antiproliferative effect of methyl-β-cyclodextrin *in vitro* and in human tumour xenografted athymic nude mice. Br. J. Cancer 78, 1165–1169.
Hueber, A.O., Bernard, A.M., Herincs, Z., Couzinet, A., He, H.T., 2002. An essential role for membrane rafts in the initiation of Fas/CD95-triggered cell death in mouse thymocytes. EMBO Rep. 3, 190–196.
Irie, T., Uekama, K., 1997. Pharmaceutical applications of cyclodextrins. III. Toxicological issues and safety evaluation. J. Pharm. Sci. 86, 147–162.
Irie, T., Uekama, K., 1999. Cyclodextrins in peptide and protein delivery. Adv. Drug Deliv. Rev. 36, 101–123.
Kondo, Y., Kanzawa, T., Sawaya, R., Kondo, S., 2005. The role of autophagy in cancer development and response to therapy. Nat. Rev. Cancer 5, 726–734.
Lacour, S., Hammann, A., Grazide, S., Lagadic-Gossmann, D., Athias, A., Sergent, O., Laurent, G., Gambert, P., Solary, E., Dimanche-Boitrel, M.T., 2004. Cisplatin-induced CD95 redistribution into membrane lipid rafts of HT29 human colon cancer cells. Cancer Res. 64, 3593–3598.
Lavrik, I.N., Golks, A., Krammer, P.H., 2005. Caspases: pharmacological manipulation of cell death. J. Clin. Invest. 115, 2665–2672.
Le Roy, C., Wrana, J.L., 2005. Clathrin- and non-clathrin-mediated endocytic regulation of cell signalling. Nat. Rev. Mol. Cell Biol. 6, 112–126.
Legler, D.F., Micheau, O., Doucey, M.A., Tschopp, J., Bron, C., 2003. Recruitment of TNF receptor 1 to lipid rafts is essential for TNF-α-mediated NF-κB activation. Immunity 18, 655–664.
Mejillano, M., Yamamoto, M., Rozelle, A.L., Sun, H.Q., Wang, X., Yin, H.L., 2001. Regulation of apoptosis by phosphatidylinositol 4,5-bisphosphate inhibition of caspases, and caspase inactivation of phosphatidylinositol phosphate 5-kinases. J. Biol. Chem. 276, 1865–1872.
Motoyama, K., Arima, H., Toyodome, H., Irie, T., Hirayama, F., Uekama, K., 2006. Effect of 2,6-di-O-methyl-α-cyclodextrin on hemolysis and morphological change in rabbit's red blood cells. Eur. J. Pharm. Sci. 29, 111–119.
Motoyama, K., Kameyama, K., Onodera, R., Araki, N., Hirayama, F., Uekama, K., Arima, H., 2009a. Involvement of PI3K-Akt-Bad pathway in apoptosis induced by 2,6-di-O-methyl-β-cyclodextrin, not 2,6-di-O-methyl-α-cyclodextrin, through cholesterol depletion from lipid rafts on plasma membranes in cells. Eur. J. Pharm. Sci. 38, 249–261.
Motoyama, K., Toyodome, H., Onodera, R., Irie, T., Hirayama, F., Uekama, K., Arima, H., 2009b. Involvement of lipid rafts of rabbit red blood cells in morphological changes induced by methylated β-cyclodextrins. Biol. Pharm. Bull. 32, 700–705.
Ohtani, Y., Irie, T., Uekama, K., Fukunaga, K., Pitha, J., 1989. Differential effects of α-, β- and γ-cyclodextrins on human erythrocytes. Eur. J. Biochem. 186, 17–22.

Onodera, R., Motoyama, K., Arima, H., 2011. Design and evaluation of folate-appended methyl-β-cyclodextrin as a new antitumor agent. J. Incl. Phenom. Macrocycl. Chem. 70, 321–326.
Rosenbaum, A.I., Zhang, G., Warren, J.D., Maxfield, F.R., 2010. Endocytosis of β-cyclodextrins is responsible for cholesterol reduction in Niemann–Pick type C mutant cells. Proc. Natl. Acad. Sci. U.S.A. 107, 5477–5482.
Shimizu, S., Matsuoka, Y., Shinohara, Y., Yoneda, Y., Tsujimoto, Y., 2001. Essential role of voltage-dependent anion channel in various forms of apoptosis in mammalian cells. J. Cell Biol. 152, 237–250.
Shimizu, S., Narita, M., Tsujimoto, Y., 1999. Bcl-2 family proteins regulate the release of apoptogenic cytochrome c by the mitochondrial channel VDAC. Nature 399, 483–487.
Simons, K., Toomre, D., 2000. Lipid rafts and signal transduction. Nat. Rev. Mol. Cell Biol. 1, 31–39.
Taatjes, D.J., Sobel, B.E., Budd, R.C., 2008. Morphological and cytochemical determination of cell death by apoptosis. Histochem. Cell Biol. 129, 33–43.
Uekama, K., Hirayama, F., Irie, T., 1998. Cyclodextrin drug carrier systems. Chem. Rev. 98, 2045–2076.
Yang, E., Zha, J., Jockel, J., Boise, L.H., Thompson, C.B., Korsmeyer, S.J., 1995. Bad, a heterodimeric partner for Bcl-XL and Bcl-2, displaces Bax and promotes cell death. Cell 80, 285–291.
Zha, J., Harada, H., Yang, E., Jockel, J., Korsmeyer, S.J., 1996. Serine phosphorylation of death agonist BAD in response to survival factor results in binding to 14-3-3 not BCL-X(L). Cell 87, 619–628.

SCIENTIFIC REPORTS

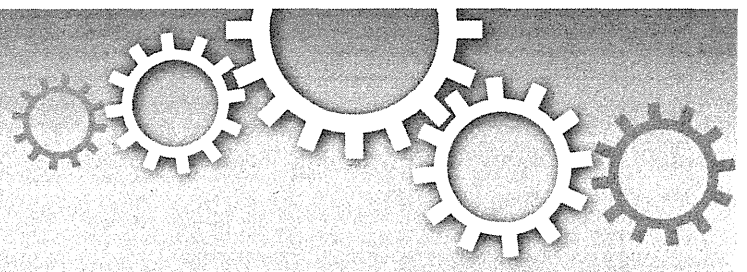

OPEN

SUBJECT AREAS:
TARGETED THERAPIES
CHEMOTHERAPY
CANCER IMMUNOTHERAPY
DRUG DEVELOPMENT

Received
2 July 2013

Accepted
4 March 2014

Published
20 March 2014

Correspondence and requests for materials should be addressed to H.A. (arimah@gpo.kumamoto-u.ac.jp)

Involvement of Autophagy in Antitumor Activity of Folate-appended Methyl-β-cyclodextrin

Risako Onodera[1], Keiichi Motoyama[1], Nao Tanaka[1], Ayumu Ohyama[1,3], Ayaka Okamatsu[1], Taishi Higashi[1], Ryusho Kariya[2], Seiji Okada[2] & Hidetoshi Arima[1,3]

[1]Department of Physical Pharmaceutics, Graduate School of Pharmaceutical Sciences, Kumamoto University, 5-1 Oe-honmachi, Chuo-ku, Kumamoto 862-0973, Japan, [2]Division of Hematopoiesis, Center for AIDS Research, Kumamoto University, 2-2-1 Honjo, Chuo-ku, Kumamoto 860-0811, Japan, [3]Program for Leading Graduate Schools "HIGO (Health life science: Interdisciplinary and Glocal Oriented) Program", Kumamoto University.

Autophagy, the major lysosomal pathway for recycling intracellular components including organelles, is emerging as a key process regulating tumorigenesis and cancer therapy. Most recently, we newly synthesized folate-appended methyl-β-cyclodextrin (FA-M-β-CyD), and demonstrated the potential of FA-M-β-CyD as a new antitumor drug. In this study, we investigated whether anticancer activity of FA-M-β-CyD in folate receptor-α (FR-α)-positive tumor cells is involved in autophagy. In contrast to methyl-β-cyclodextrin (M-β-CyD), FA-M-β-CyD entered KB cells (FR-α (+)) through CLIC/GEEC endocytosis. No significant depression in the DNA content was observed in KB cells after treatment with FA-M-β-CyD. Additionally, the transmembrane potential of mitochondria after treatment with FA-M-β-CyD was drastically elevated. Meanwhile, FA-M-β-CyD induced the formation of autophagic vacuoles, which were partially colocalized with mitochondria, in KB cells. Taken together, these results suggest that FR-α-expressing cell-selective cytotoxic activity of FA-M-β-CyD could be mediated by the regulation of autophagy, rather than the induction of apoptosis.

In cancer chemotherapy, to obtain the maximum treatment efficacy of anticancer agents, the drug delivery technique is extremely important. To confer an active targeting-ability, the chemical modification of tumor-specific ligands to a drug carrier is known. Of various tumor-specific ligands, folic acid (FA)[1–5] has emerged as a remarkable targeting ligand capable of potent interaction with cancer cells expressing the folate receptor (FR) with high affinity (K_d: $10^{-9} \sim 10^{-10}$ M)[6,7]. FR is engaged the cell surface through a glycosylphosphatidylinositol-anchor, and is highly expressed in various tumor cells including malignancies of the brain, ovary, breast, kidney, and lung, and has negligible expression in normal tissues[8]. In addition, as a cancer progress, the expression level of FR increase remarkably[9]. Therefore, FR is one of the potent candidate for not only a promising marker but also a target protein for therapy of cancer.

Cyclodextrins (CyDs) are cyclic oligosaccharides forming inclusion complexes with a wide range of hydrophobic molecules, and are used widely in pharmaceutical region[10,11]. CyDs have been reported to interact with cell membrane components of cholesterol and phospholipids, resulting in the induction of hemolysis of red blood cells at high concentrations of CyDs[12–14]. In Addition, methyl-β-cyclodextrin (M-β-CyD) is often used to disrupt lipid rafts because of its ability to decrease cholesterol stores on cell membranes[15]. A number of studies have also demonstrated that the disruption of lipid rafts by M-β-CyD can harm cancer cells and cause cell-death. Notedly, Grosse *et al.* revealed that M-β-CyD significantly reduced tumor growth in tumor-bearing mice after intraperitoneal administration[16]. However, the cytotoxic reaction of M-β-CyD has a lack of a tumor cell-selectivity.

Most recently, to make an attempt to give a tumor-specific cytotoxic reaction to M-β-CyD, we previously prepared FA-conjugated M-β-CyD (FA-M-β-CyD)[17], and evaluated its antitumor activity[18]. FA-M-β-CyD provided great antitumor activity, compared to M-β-CyD in KB cells, highly expressing folate receptor-α (FR-α). The single intravenous administration of FA-M-β-CyD significantly suppressed the tumor growth in Colon-26 cells (FR-α (+))-bearing mice. Additionally, the antitumor activity of FA-M-β-CyD was superior to that of doxorubicin after an intravenous administration, at the same dose. These results indicate that FA-M-β-CyD has the potential as a promising anticancer agent. However, the mechanism of antitumor activity of FA-M-β-CyD still remains unclear.

Autophagy, the major lysosomal pathway for recycling intracellular components including organelles, is emerging as a key process regulating tumorigenesis and cancer therapy[19–23]. The dynamic roles for autophagy in cancer is tumor suppressive effect in the early stage of cancer development, but is the growth effect of established tumors. Likewise, the stimulation of autophagy in response to therapeutics can contextually favor or weaken chemoresistance and antitumor immunity. Therefore, the understanding whether and how autophagy can be harnessed to kill cancer cells is essential for cancer chemotherapy. In this study, we investigated whether antitumor activity of FA-M-β-CyD in FR-α (+) cells is involved in autophagy. As a result, FA-M-β-CyD was found to induce autophagosome formation in FR-α (+) cells, indicating the involvement of autophagy in antitumor activity. Taking into the consideration of our previous results that FA-M-β-CyD drastically suppressed the tumor growth in mice inoculated FR-α (+) tumor cells[18], FA-M-β-CyD can be applied as a novel anticancer drug through regulating autophagy for cancer chemotherapy against FR-α-overexpressing tumor.

Results

Antitumor effect of FA-M-β-CyD. To elucidate the antitumor effect of FA-M-β-CyD in FR-α (+) cells, we investigated antitumor effect of FA-M-β-CyD in FR-α (+) and FR-α (−) cells. FA-M-β-CyD had great antitumor effect in FR-α (+) cells such as KB and M213 cells, compared to control, after treatment for 2 h (Fig. 1A, B). However, there was no significant antitumor activity in FR-α-negative A549 cells (Fig. 1C). These results indicate that FA-M-β-CyD had FR-α (+) cell-selective antitumor effect.

Cellular association and intracellular distribution of FA-M-β-CyD. Previously, we reported that FA-M-β-CyD possesses FR-α (+) cell-specific antitumor effect[18]. To obtain the detail of the mechanism for the FR-α-mediated antitumor effect of FA-M-β-CyD, we studied whether TRITC-FA-M-β-CyD associates with KB cells (Fig. 2). Strikingly, TRITC-FA-M-β-CyD highly associated with KB cells (Fig. 2A), despite CyDs are known to be biomembrane-impermeable. Furthermore, the association of TRITC-FA-M-β-CyD was inhibited by the addition of FA as a competitor of FR (Fig. 2A). Similar results were observed in M213 cells (Fig. 2B). Additionally, cellular association of FA-M-β-CyD was significantly lowered in FR-α down-regulated KB cells, compared to KB cells (Fig. 2C). These data indicate that FA-M-β-CyD could associate with cells through FR-α.

Next, we examined the intracellular distribution of TRITC-FA-M-β-CyD in KB cells after 1 h treatment (Fig. 3). It should be noted that cellular uptake of TRITC-FA-M-β-CyD in KB cells was observed. Furthermore, TRITC-FA-M-β-CyD mainly localized in cytoplasm rather than in nucleus after 1 h treatment. Collectively, these results indicate that FA-M-β-CyD distributed in cytoplasm after the cellular uptake into KB cells, and provided potent antitumor effects.

FA-M-β-CyD caused cytotoxic activity via apoptosis-independent pathway. To examine whether FA-M-β-CyD induces apoptosis or not, we investigated the DNA content in nucleus, transmembrane potential in mitochondria, TUNEL assay, and caspase 3 cleavage assay in KB cells. Here, we used 2, 6-di-*O*-methyl-β-CyD (DM-β-CyD) as a positive control of apoptosis inducer, because we previously demonstrated that DM-β-CyD elicited apoptosis through the suppression of the PI3K-Akt activity, through cholesterol extraction from plasma membranes in NR8383 cells[24]. The DNA content in KB cells after treatment with 10 mM DM-β-CyD for 2 h was significantly lowered, compared to that with control (Fig. 4A). Meanwhile, no significant decrease in the DNA content was observed in 10 mM FA-M-β-CyD in KB cells (Fig. 4A).

Next, we investigated the effects of CyDs on transmembrane potential in mitochondria using rhodamine 123 in KB cells (Fig. 4B). The transmembrane potential in mitochondria of KB cells treated with DM-β-CyD was drastically decreased, compared to control. In sharp contrast, the potential of KB cells treated with FA-M-β-CyD was drastically elevated. Furthermore, this increment of the potential by the addition of FA-M-β-CyD was decreased to control level in the presence of FA, a competitor of FR (Fig. 4B).

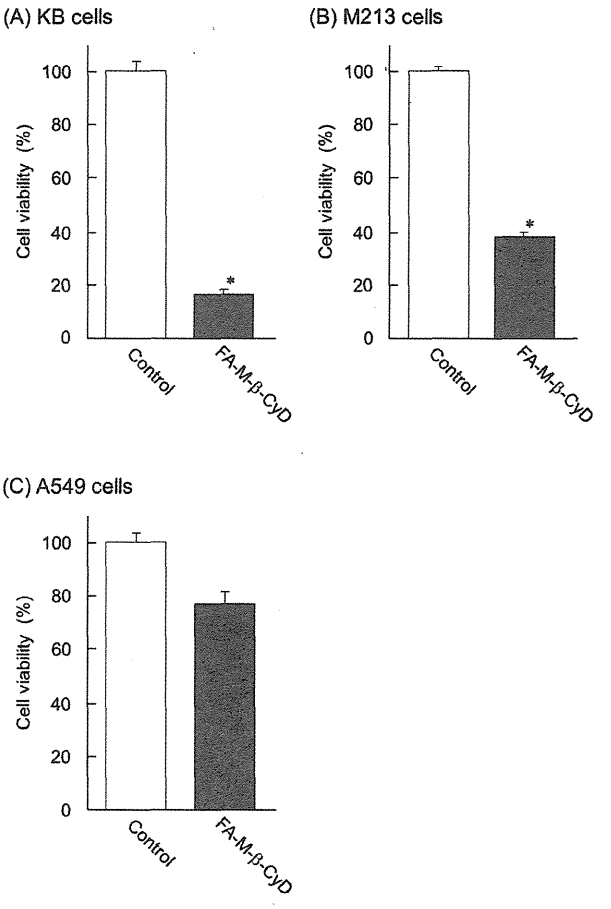

Figure 1 | Antitumor effect of FA-M-β-CyD. (A) KB cells, (B) M213 cells, and (C) A549 cells. The concentration of FA-M-β-CyD was 10 mM. Results are represented as mean ± S.E.M. (n = 3–4 per group). $*p < 0.05$ vs. control.

Next, we performed TUNEL assay. As shown in Fig. 4C, KB cells treated with DM-β-CyD were stained, compared to control, suggesting the induction of apoptosis. Meanwhile, the cells treated with FA-M-β-CyD were not stained.

Furthermore, in the cleaved caspase 3 assay (Fig. 4D, 4E), DM-β-CyD potently produced activated-caspase 3 through a cleavage of pro-caspase 3, indicating the induction of apoptosis. However, FA-M-β-CyD showed only slight cleavage activity for pro-caspase 3. Collectively, these data indicate that cell-death caused by FA-M-β-CyD was apoptosis-independent.

Involvement of autophagy in cell-death caused by FA-M-β-CyD. Autophagy is a normal physiological process in the body that deals with destruction of cells in the body, and can kill the cells under certain conditions. There are several reports on autophagy or autophagic cell-death activated in cancer cells after treatment with various anticancer drugs[25]. Next, we examined whether autophagosome formation in KB cells is elicited by FA-M-β-CyD, using Cyto-ID® Autophagy Detection Kit, which detects autophagic vacuoles in cells. As shown in Fig. 5A and 5B, the autophagic

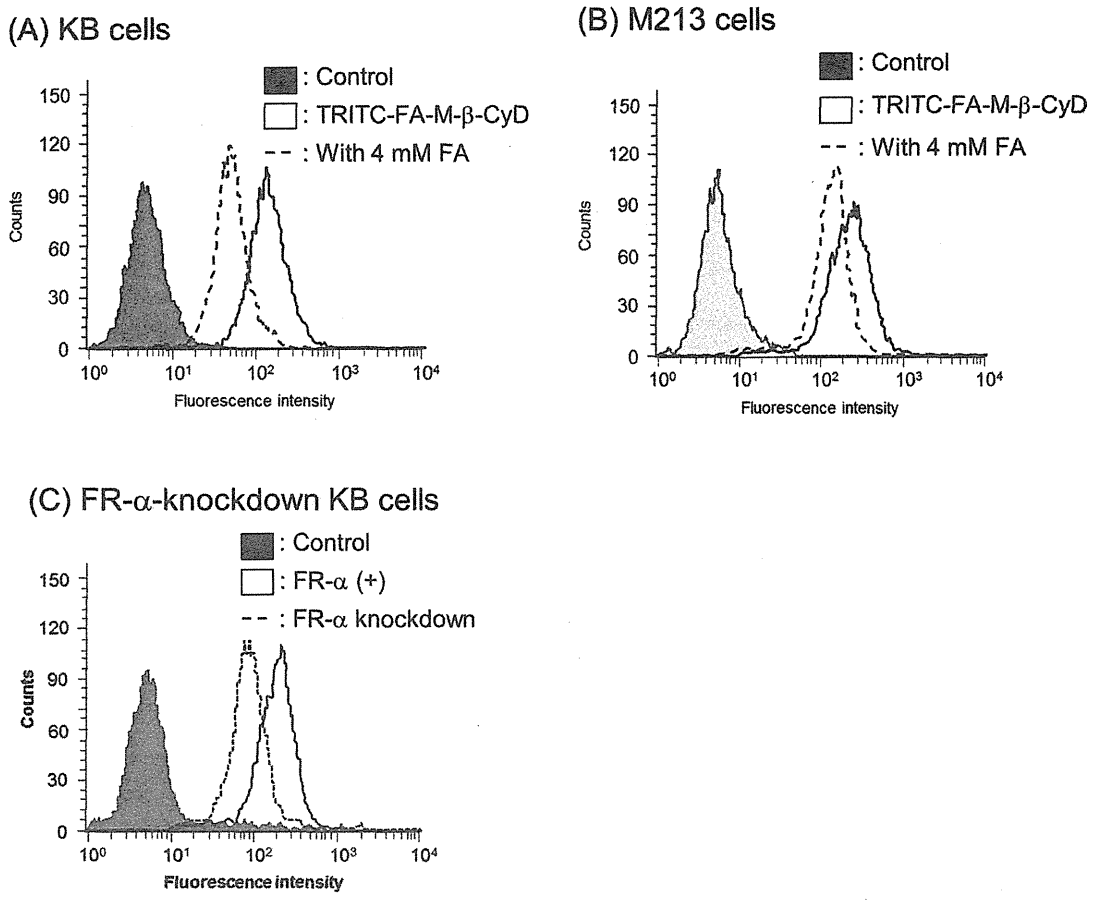

Figure 2 | Cellular association of TRITC-FA-M-β-CyD. (A) KB cells, (B) M213 cells and (C) FR-α-knockdown cells. The fluorescence intensity derived from TRITC was determined 1 h after incubation at 37°C by a flow cytometer.

vacuoles in KB cells were observed after treatment with FA-M-β-CyD for 2 h. Additionally, the autophagic vacuoles elicited by the treatment with FA-M-β-CyD were overwhelmingly decreased by the pretreatment of LY294002, an autophagy inhibitor. These results suggest that FA-M-β-CyD induced the formation of autophagic vacuoles in KB cells.

Next, we performed autophagy assay using a kit of Premo™ Autophagy Sensors, which can monitor a clearance of protein aggregates via autophagy using GFP-labeled p62 in Fig. 5C and 5D. Here, the p62 protein is able to bind to both ubiquitin[26] and LC3[27], thereby facilitating clearance of ubiquitinated proteins via autophagy. The fluorescence of GFP-p62 in control was drastically lowered by the addition of FA-M-β-CyD. Meanwhile, M-β-CyD did not show significant change in the fluorescence of GFP-p62, compared to control. These results suggest that the accumulated autophagosomes in KB cells were degraded by FA-M-β-CyD via autophagy.

Next, we examined the effects of autophagy inhibitors such as chloroquine, bafilomycin A1, 3-methyladenine (3-MA), and LY294002 on cell viability of KB cells after treatment with FA-M-β-CyD. Here, chloroquine and bafilomycin A1 prevent endosomal acidification, which leads to inhibition of both fusion of autophagosome with lysosome and lysosomal protein degradation. 3-MA and

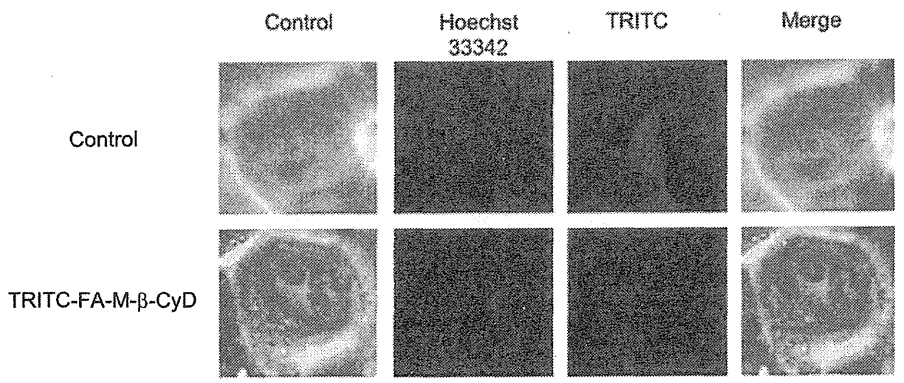

Figure 3 | Intracellular distribution of TRITC-FA-M-β-CyD. KB cells were treated with TRITC-FA-M-β-CyD (10 μM) for 1 h.

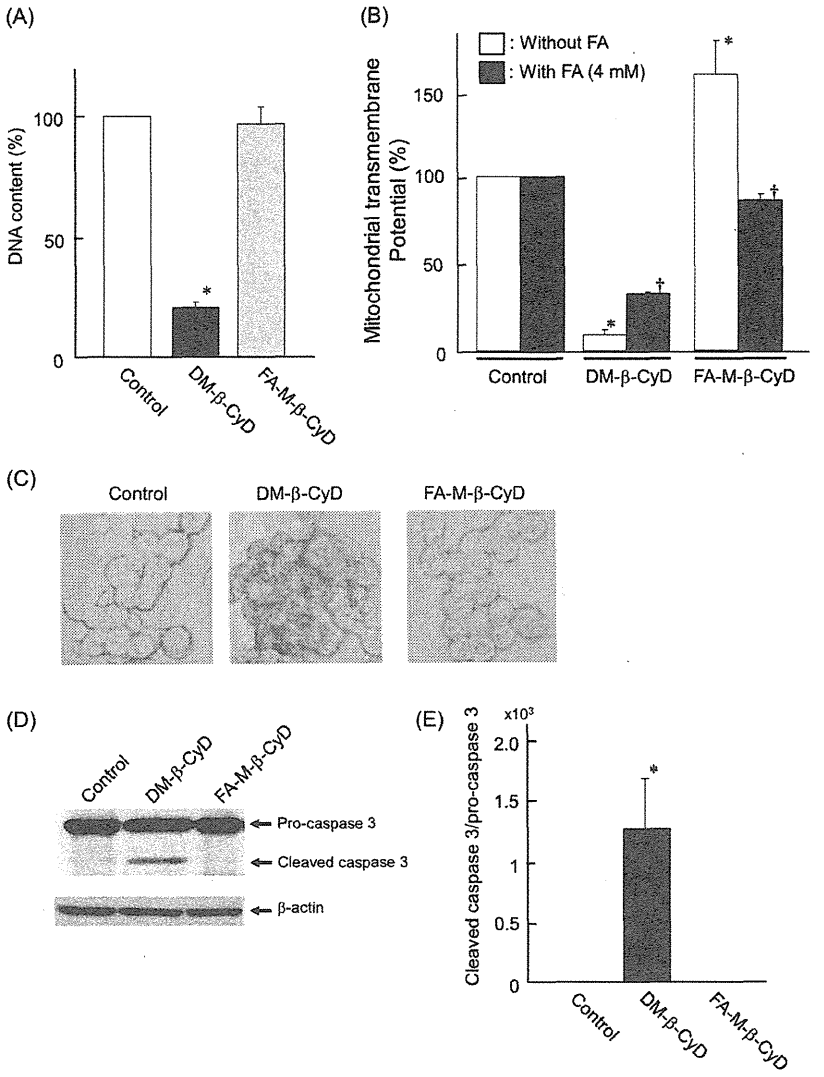

Figure 4 | DNA content (A) and mitochondrial transmembrane potential (B) after treatment with FA-M-β-CyD. KB cells were treated with FA-M-β-CyD (10 mM) for 2 h. Results are represented as mean ± S.E.M. (n = 3–4 per group). $*p < 0.05$ vs. control. $\dagger p < 0.05$ vs. KB cells without treatment of FA. (C) TUNEL assay after treatment with FA-M-β-CyD in KB cells. (D) Cleaved caspase 3 assay after treatment with FA-M-β-CyD in KB cells. The cropped blots were indicated. (E) The band intensity of cleaved caspase 3/pro-caspase 3 ratio. Results are represented as mean ± S.E.M. (n = 3 per group). $*p < 0.05$ vs. control.

LY294002 were used as PI3K inhibitors. As shown in Fig. 5E, the cell viability of KB cells treated with FA-M-β-CyD in the presence of autophagy inhibitors was higher than that with FA-M-β-CyD alone. Taken together, these data indicate that FA-M-β-CyD is likely to cause autophagic cell-death.

The dysfunctional mitochondria are recognized and degraded within cells by both non-selective autophagy and mitophagy, a selective type of autophagy[28,29]. As shown in Fig. 4B, we found that FA-M-β-CyD significantly enhanced the mitochondrial membrane potential in KB cells, indicating the induction of mitochondrial stress. Therefore, we examined the involvement of mitophagy in cell-death caused by mitochondrial stress after treatment with FA-M-β-CyD (Fig. 6). The autophagic vacuoles and mitochondria, stained by Cyto-ID® Autophagy Detection Kit and rhodamine 123, respectively, were partially colocalized in KB cells after treatment with FA-M-β-CyD (Fig. 6A). Similar results were obtained in M213 cells (Fig. 6B). Therefore, these results suggest that the autophagic cell-death induced by FA-M-β-CyD could be associated with mitophagy elicited by a mitochondrial stress.

Discussion

Having a targeting ability of antitumor agents plays a key role to not only provide strong antitumor activity but also reduce a risk of side effects in cancer chemotherapy. Previously, we demonstrated that FA-M-β-CyD showed a FR-α (+) cell-selective antitumor effect[17]. Additionally, we revealed that the antitumor effect of FA-M-β-CyD was significantly suppressed in the presence of FA, indicating that FR-mediated endocytosis is crucial for the enhancement of antitumor effect by FA-M-β-CyD[18]. In generally, it is believed that the extent of cellular uptake of CyDs is negligible probably due to their hydrophilicity and high molecular weight, FA-M-β-CyD was actually internalized into KB cells (Fig. 3). Meanwhile, FR was thought to be endocytosed via clathrin-independent carrier/GPI-anchored proteins enriched early endosomal compartment (CLIC/GEEC)[30]. Therefore, FA-M-β-CyD could enter the cells via CLIC/GEEC after the recognition by FR-α. Actually, FA-M-β-CyD highly associated with KB cells rather than that with FR-α-knockdown KB cells (Fig. 2C), indicating the potential of FA-M-β-CyD as a FR-α (+) cell-selective anticancer drug.

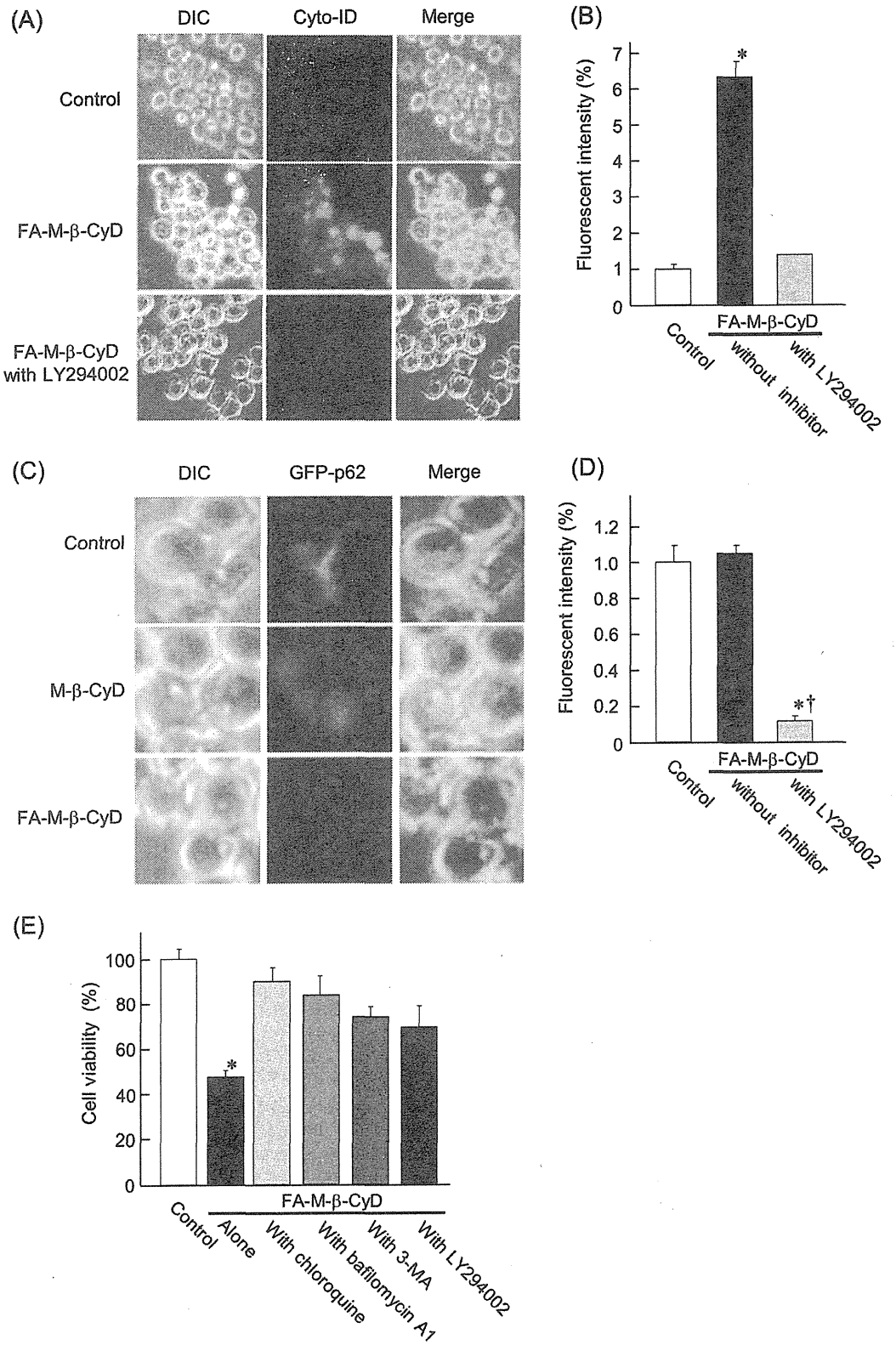

Figure 5 | Induction of autophagy by the treatment of FA-M-β-CyD. (A, B) Effects of FA-M-β-CyD on the autophagosome formation in KB cells. (C, D) Effects of FA-M-β-CyD on the clearance of protein aggregation via autophagy. (E) Effects of chloroquine, bafilomycin A1, 3-MA, and LY294002 on antitumor activity of FA-M-β-CyD for KB cells. Results are represented as mean ± S.E.M. (n = 3–6 per group). *$p < 0.05$ vs. control. †$p < 0.05$ vs. FA-M-β-CyD without inhibitor.

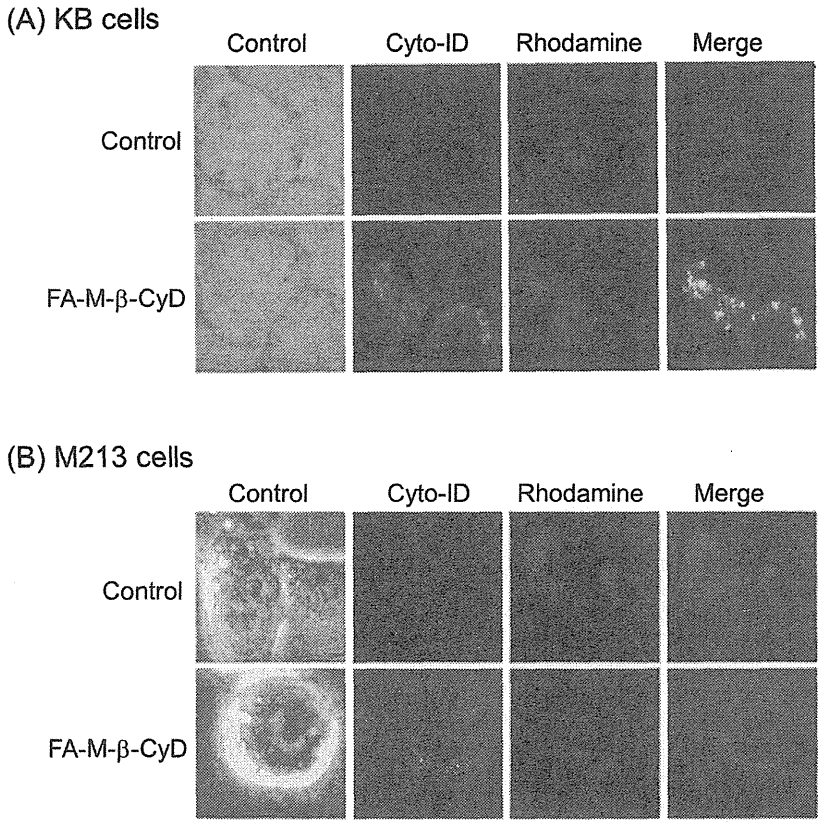

Figure 6 | Colocalization of autophagosomes and mitochondria in KB cells and M213 cells after treatment with FA-M-β-CyD. (A) KB cells and (B) M213 cells were treated with FA-M-β-CyD for 2 h, and then the cells were treated with Cyto-ID™ and rhodamine 123, to stain autophagosomes and mitochondria, respectively.

Recently, an alternative process for controlling cell-death and novel drugs eliciting cancer cell demise have been discovered[31]. Among cell-death machinery, apoptosis plays crucial roles in cell survival and tumor growth. M-β-CyD is often utilized to impair lipid rafts due to the extraction of cholesterol from plasma membranes[15,32]. A number of studies have revealed that M-β-CyD can harm cancer cells through the impairment of lipid rafts. For instance, the decrease in cholesterol level by M-β-CyD provoked apoptosis in human epidermoid carcinoma cells[33]. In addition, we previously reported that DM-β-CyD elicited apoptosis by the impairment of the PI3K-Akt activity, through the depletion of cholesterol from lipid rafts in alveolar macrophages[24]. We also verified that DM-β-CyD provided apoptosis in KB cells through cholesterol depletion (Fig. 4). Additionally, M-β-CyD also elicited apoptosis in KB cells, due to the cholesterol extraction, leading to lowering DNA content in nucleus and transmembrane potential in mitochondria[34]. Interestingly, FA-M-β-CyD significantly released cholesterol from both KB cells (FR-α (+)) and A549 cells (FR-α (−)) to culture medium, compared to that of M-β-CyD and DM-β-CyD in our previous study[18]. However, FA-M-β-CyD showed potent cytotoxic activity without reducing the DNA content in nucleus and transmembrane potential in mitochondria (Fig. 4), suggesting that the cell-death mechanism in FA-M-β-CyD system could be different from apoptosis. Taken together, the modification of FA to M-β-CyD drastically changed the cell-death mechanism, probably due to entry into FR-α-overexpressing cells mediated by CLIC/GEEC endocytosis.

Most importantly, we revealed that involvement of autophagy in cell-death caused by FA-M-β-CyD in FR-α-expressing cells such as KB cells. That is, FA-M-β-CyD enhanced the expression of LC3-II, an autophagosome marker, in autophagic membranes in KB cells (Fig. 5A). Recently, autophagy is thought to be emerging as a key process regulating tumorigenesis and cancer therapy. At the early stage of tumor development, autophagy functions as a tumor suppressor. Meanwhile, at advanced stages of tumor development, autophagy promotes tumor progression. The tumor cells that are located in the central area of the tumor mass undergo autophagy to survive under low-oxygen and low-nutrient conditions. Autophagy protects some cancer cells against anticancer treatment by blocking the apoptotic pathway ('protective autophagy'). In the present study, FA-M-β-CyD was found to induce autophagosome formation in FR-α-positive cells, suggesting the involvement of autophagy in antitumor activity. Taking into the consideration of our previous results that FA-M-β-CyD drastically suppressed the tumor growth in mice inoculated FR-α (+) tumor cells[18], FA-M-β-CyD can be applied as a novel anticancer drug through regulating autophagy for cancer chemotherapy against FR-α-overexpressing tumor. However, it still remains unclear whether FA-M-β-CyD induces the dephosphorylation and inactivation of mTOR, which elicits autophagy, and activates class III PI3K, which involves in the autophagosome formation. Therefore, the further studies on not only the mechanism of autophagy caused by FA-M-β-CyD, but also the contribution of endocytosis pathway to cell-death mechanism are required.

Activation of mitochondrial permeability pore (mPTP) is associated with mitochondrial depolalization, uncoupling of oxidative dephosphorylation, swelling of mitochondria and release of death-promoting factors like cytochrome *c*[35]. Recently, Ziolkowski *et al.* demonstrated that M-β-CyD decreases the function of rat liver mitochondria, and suppresses the calcium chloride-induced swelling[36]. In the present study, FA-M-β-CyD internalized into KB cells may

interact with mitochondrial raft-like microdomains, leading to the suppression of mPTP activity, resulting in the regulation of autophagosome formation. Further elaborate studies regarding the effects of FA-M-β-CyD on mitochondrial function are in progress.

In conclusion, in the present study, we revealed the involvement of autophagy in FR-α-expressing cell-selective antitumor effect of FA-M-β-CyD. These finding will give great information of FA-M-β-CyD as a novel autophagy inducer for cancer chemotherapy.

Methods

Materials. RPMI-1640 (FA-free) was obtained from GIBCO (Tokyo, Japan). Tetramethylrhodamine isothiocyanate (TRITC) and FR-α siRNA (sc-39969) were purchased from Funakoshi (Tokyo, Japan) and Santa Cruz Biotechnology (Delaware, CA), respectively. Lipofectamine™2000 reagent and Premo™ Autophagy Sensors were obtained from Invitrogen (Tokyo, Japan). Cyto-ID® Autophagy Detection Kit was purchased from Enzo Life Sciences (Farmingdale, NY).

Cell culture and *In vitro* antitumor activity. KB cells, a human oral squamous carcinoma cell line, A549 cells, a human lung carcinoma, and M213 cells, a human cholangiocarcinoma cell line, were cultured as reported previously[17]. The antitumor activity *in vitro* was performed by the WST-1 method, as reported previously[18]. Briefly, KB cells, M213 cells and A549 cells (5×10^4/96-well microplate) were treated with 150 μL of culture medium containing 10 mM FA-M-β-CyD for 2 h at 37°C. In the autophagy inhibitory study, KB cells were pretreated with RPMI-1640 culture medium containing 20 μM chloroquine, 1 nM bafilomycin A1, 5 mM 3-methyladenine (3-MA), and 50 μM LY294002 for 24 h. After washing with PBS (pH 7.4), 100 μL of fresh HBSS (pH 7.4) was supplemented. Then, the plates and incubated with WST-1 reagent for 30 min. The absorption wavelength and reference wavelength were 450 nm and 630 nm, respectively.

Cellular association of FA-M-β-CyD. KB cells and M213 cells (1×10^6/35 mm dish) were incubated with 1 mL of culture medium (FA-free) containing 10 μM tetramethylrhodamine isothiocyanate (TRITC)-labeled FA-M-β-CyD (TRITC-FA-M-β-CyD) at 37°C for 1 h. After washing with PBS (pH 7.4), the cells were scraped with 1 mL of PBS (pH 7.4). Data were obtained for 1×10^4 cells on a FACS Calibur flow cytometer using CellQuest software (Becton-Dickinson, Mountain View, CA).

Intracellular distribution of FA-M-β-CyD. KB cells (1×10^6/35 mm glass bottom dish) were treated with 10 μM TRITC-FA-M-β-CyD at 37°C for 1 h. Hoechst 33342 (10 μg/mL) was incubated at 37°C for 10 min. After washing with PBS (pH7.4), RPMI-1640 (FA-free) was added. KEYENCE Biozero BZ-8000, a fluorescence microscope, was used for the detection of TRITC and Hoechest33342.

DNA content and mitochondrial transmembrane potential. The DNA content and transmembrane potential in mitochondria in KB cells were determined as reported previously[34]. Briefly, KB cells (1×10^6/35 mm dish) were treated with RPMI-1640 (FA-free) containing 10 mM DM-β-CyD or FA-M-β-CyD for 2 h. Propidium iodide (PI, 20 μg/mL) and rhodamine 123, the indicators of DNA content and transmembrane potential in mitochondria, respectively, were quantified using a FACS Calibur flow cytometer with CellQuest software.

TUNEL assay. Detection of apoptosis was done by TUNEL assay. In short, KB cells (1×10^6/35 mm glass bottom dish) were incubated with 5 mM DM-β-CyD or FA-M-β-CyD at 37°C for 1 h. The cells were washed with PBS and fixed by incubation in 4% paraformaldehyde in PBS for 1 hr at room temperature. Terminal deoxynucleotidyl transferase (TdT)-mediated dUTP nick and labeling (TUNEL) assays were performed by using the TACS® 2 TdT-DAB in situ Apoptosis Detection Kit (Trevigen Inc., Gaithersburg, MD) according to the manufacturer's instructions.

Cleaved caspase 3 assay. Caspase 3 cleavage assay was performed by western blotting. Briefly, KB cells (1×10^6/35 mm dish) were incubated with RPMI-1640 culture medium (FA-free) containing 10 mM DM-β-CyD or FA-M-β-CyD for 2 h. After washed with PBS, cells were lysed with 4× sample buffer (8% SDS, 40% glycerol, 24% β-mercaptoethanol in Tris-HCl buffer (pH6.8)) and boiled for 5 min. After determining protein concentrations using the bicinchoninic acid reagent from Pierce Chemical (Rockford, IL), samples (20 μg as proteins) were separated with 12% SDS-PAGE and transferred onto Immobilon P membranes (Nihon Millipore, Tokyo, Japan). The membranes were blocked with 5% skim milk in PBS containing 0.1% Tween 20 (PBS-T) and incubated with caspase 3 antibody (Santa Cruz, Delaware, CA) at 4°C for overnight. After washing with PBS-T, the membranes were incubated with secondary antibody of peroxidase-conjugated sheep (Amersham-pharmacia Biotech, Buckinghamshire, UK). Specific bands were detected using an ECL Western blotting analysis kit (Amersham Bioscience, Tokyo, Japan). The bands were detected using the Lumino-image analyzer LAS-1000 plus (Fujifilm, Tokyo, Japan). The band intensity ratio of cleaved caspase 3/pro-caspase 3 was analyzed by Image-J software.

Autophagosome formation. Briefly, KB cells (1×10^6/35 mm dish) were incubated with FA-M-β-CyD (5 mM) for 2 h, in the presences and absence of pretreatment with 1 μM LY294002, an autophagic inhibitor, for 4 h, and then the cells were treated with Cyto-ID® Autophagy Detection Kit. A fluorescence microscope of Biozero BZ-8000 (KEYENCE) was used for cell observation.

Clearance of protein aggregates via autophagy. The clearance of protein aggregates via autophagy was evaluated by the Premo™ Autophagy Sensors. Briefly, the cells (5×10^5/35 mm glass bottom dish) were incubated with RPMI-1640 culture medium (FA-free) for 24 h. After washing with PBS, 25 μL of GFP-p62 was added to the culture medium. After incubation for 16 h, the cells were washed with PBS and incubated with 50 μM chloroquine for 10 h. Then, the cells were incubated with 5 mM FA-M-β-CyD in the presence of 50 μM chloroquine for 2 h. After washing with RPMI-1640 culture medium (FA-free), a fluorescence microscope of Biozero BZ-8000 (KEYENCE) was used for cell observation.

Statistics. All experiments were performed in triplicate in each series of measurements, and each series was repeated more than three times. The experimental results are shown as means ± S.E.M. Significance levels for comparisons between samples were determined with Scheffe's test. The level of statistical significance was set at $P < 0.05$.

1. Chen, H., Ahn, R., Van den Bossche, J., Thompson, D. H. & O'Halloran, T. V. Folate-mediated intracellular drug delivery increases the anticancer efficacy of nanoparticulate formulation of arsenic trioxide. *Mol. Cancer Ther.* **8**, 1955–1963 (2009).
2. Gabizon, A. *et al.* Improved therapeutic activity of folate-targeted liposomal doxorubicin in folate receptor-expressing tumor models. *Cancer Chemother. Pharmacol.* **66**, 43–52 (2010).
3. Lu, Y. & Low, P. S. Folate-mediated delivery of macromolecular anticancer therapeutic agents. *Adv. Drug Deliv. Rev.* **54**, 675–693 (2002).
4. Mi, Y., Liu, Y. & Feng, S. S. Formulation of Docetaxel by folic acid-conjugated d-α-tocopheryl polyethylene glycol succinate 2000 (Vitamin E TPGS(2k)) micelles for targeted and synergistic chemotherapy. *Biomaterials* **32**, 4058–4066 (2011).
5. Nukolova, N. V., Oberoi, H. S., Cohen, S. M., Kabanov, A. V. & Bronich, T. K. Folate-decorated nanogels for targeted therapy of ovarian cancer. *Biomaterials* **32**, 5417–5426 (2011).
6. Antony, A. C. The biological chemistry of folate receptors. *Blood* **79**, 2807–2820 (1992).
7. Low, P. S. & Kularatne, S. A. Folate-targeted therapeutic and imaging agents for cancer. *Curr. Opin. Chem. Biol.* **13**, 256–262 (2009).
8. Limmon, G. V. *et al.* Scavenger receptor class-A is a novel cell surface receptor for double-stranded RNA. *FASEB J.* **22**, 159–167 (2008).
9. Parker, N. *et al.* Folate receptor expression in carcinomas and normal tissues determined by a quantitative radioligand binding assay. *Anal. Biochem.* **338**, 284–293 (2005).
10. Szente, L. & Szejtli, J. Highly soluble cyclodextrin derivatives: chemistry, properties, and trends in development. *Adv. Drug Deliv. Rev.* **36**, 17–28 (1999).
11. Uekama, K. & Otagiri, M. Cyclodextrins in drug carrier systems. *Crit. Rev. Ther. Drug Carrier Syst.* **3**, 1–40 (1987).
12. Motoyama, K. *et al.* Effect of 2,6-di-*O*-methyl-α-cyclodextrin on hemolysis and morphological change in rabbit's red blood cells. *Eur. J. Pharm. Sci.* **29**, 111–119 (2006).
13. Motoyama, K. *et al.* Involvement of lipid rafts of rabbit red blood cells in morphological changes induced by methylated β-cyclodextrins. *Biol. Pharm. Bull.* **32**, 700–705 (2009).
14. Ohtani, Y., Irie, T., Uekama, K., Fukunaga, K. & Pitha, J. Differential effects of α-, β- and γ-cyclodextrins on human erythrocytes. *Eur. J. Biochem.* **186**, 17–22 (1989).
15. Galbiati, F., Razani, B. & Lisanti, M. P. Emerging themes in lipid rafts and caveolae. *Cell* **106**, 403–411 (2001).
16. Grosse, P. Y., Bressolle, F. & Pinguet, F. Antiproliferative effect of methyl-β-cyclodextrin *in vitro* and in human tumour xenografted athymic nude mice. *Br. J. Cancer* **78**, 1165–1169 (1998).
17. Onodera, R., Motoyama, K. & Arima, H. Design and evaluation of folate-appended methyl-β-cyclodextrin as a new antitumor agent. *J. Incl. Phenom. Macrocycl. Chem.* **70**, 321–326 (2011).
18. Onodera, R., Motoyama, K., Okamatsu, A., Higashi, T. & Arima, H. Potential use of folate-appended methyl-β-cyclodextrin as an anticancer agent. *Sci. Rep.* **3(1109)**, 1–9 (2013).
19. Liang, C. *et al.* Autophagic and tumour suppressor activity of a novel Beclin1-binding protein UVRAG. *Nat. Cell Biol.* **8**, 688–699 (2006).
20. Liu, E. Y. & Ryan, K. M. Autophagy and cancer--issues we need to digest. *J. Cell Sci.* **125**, 2349–2358 (2012).
21. Qu, X. *et al.* Promotion of tumorigenesis by heterozygous disruption of the beclin 1 autophagy gene. *J. Clin. Invest.* **112**, 1809–1820 (2003).
22. Takahashi, Y. *et al.* Bif-1 interacts with Beclin 1 through UVRAG and regulates autophagy and tumorigenesis. *Nat. Cell Biol.* **9**, 1142–1151 (2007).
23. White, E. Deconvoluting the context-dependent role for autophagy in cancer. *Nat. Rev. Cancer* **12**, 401–410 (2012).
24. Motoyama, K. *et al.* Involvement of PI3K-Akt-Bad pathway in apoptosis induced by 2,6-di-*O*-methyl-β-cyclodextrin, not 2,6-di-*O*-methyl-α-cyclodextrin, through cholesterol depletion from lipid rafts on plasma membranes in cells. *Eur. J. Pharm. Sci.* **38**, 249–261 (2009).

25. Kondo, Y., Kanzawa, T., Sawaya, R. & Kondo, S. The role of autophagy in cancer development and response to therapy. *Nat. Rev. Cancer.* **5**, 726–734 (2005).
26. Geetha, T. & Wooten, M. W. Structure and functional properties of the ubiquitin binding protein p62. *FEBS Lett.* **512**, 19–24 (2002).
27. Pankiv, S. *et al.* p62/SQSTM1 binds directly to Atg8/LC3 to facilitate degradation of ubiquitinated protein aggregates by autophagy. *J. Biol. Chem.* **282**, 24131–24145 (2007).
28. Kim, I., Rodriguez-Enriquez, S. & Lemasters, J. J. Selective degradation of mitochondria by mitophagy. *Arch. Biochem. Biophys.* **462**, 245–253 (2007).
29. Rodriguez-Hernandez, A. *et al.* Coenzyme Q deficiency triggers mitochondria degradation by mitophagy. *Autophagy* **5**, 19–32 (2009).
30. Doherty, G. J. & McMahon, H. T. Mechanisms of endocytosis. *Annu. Rev. Biochem.* **78**, 857–902 (2009).
31. Long, J. S. & Ryan, K. M. New frontiers in promoting tumour cell death: targeting apoptosis, necroptosis and autophagy. *Oncogene* **31**, 5045–5060 (2012).
32. Simons, K. & Ehehalt, R. Cholesterol, lipid rafts, and disease. *J. Clin. Invest.* **110**, 597–603 (2002).
33. Park, E. K. *et al.* Cholesterol depletion induces anoikis-like apoptosis via FAK down-regulation and caveolae internalization. *J. Pathol.* **218**, 337–349 (2009).
34. Onodera, R. *et al.* Involvement of cholesterol depletion from lipid rafts in apoptosis induced by methyl-β-cyclodextrin. *Int. J. Pharm.* **452**, 116–123 (2013).
35. Bernardi, P., Scorrano, L., Colonna, R., Petronilli, V. & Di Lisa, F. Mitochondria and cell death. Mechanistic aspects and methodological issues. *Eur. J. Biochem.* **264**, 687–701 (1999).
36. Ziolkowski, W. *et al.* Methyl-β-cyclodextrin induces mitochondrial cholesterol depletion and alters the mitochondrial structure and bioenergetics. *FEBS Lett.* **584**, 4606–4610 (2010).

Acknowledgments

This work was funded by a Japan Society for the Promotion of Science (Grant-in-Aid for Young Scientists (B) (25870537)), a Ministry of Health Labour and Welfare (Grant-in-Aid for Third Term Comprehensive Control Research for Cancer program (24100701)), and The Japan Science Society (Sasakawa Scientific Research Grant).

Author contributions

R.O., K.M., N.T., A.O. and A.O. performed the experiments. R.O., K.M., T.H., R.K., S.O. and H.A. analysed the data. R.O., K.M. and H.A. designed the research. K.M., R.O. and H.A. wrote this manuscript. H.A. supervised this work.

Additional information

Supplementary information accompanies this paper at http://www.nature.com/scientificreports

Competing financial interests: The authors declare no competing financial interests.

How to cite this article: Onodera, R. *et al.* Involvement of Autophagy in Antitumor Activity of Folate-appended Methyl-β-cyclodextrin. *Sci. Rep.* **4**, 4417; DOI:10.1038/srep04417 (2014).

This work is licensed under a Creative Commons Attribution-NonCommercial-NoDerivs 3.0 Unported license. To view a copy of this license, visit http://creativecommons.org/licenses/by-nc-nd/3.0